Inorg. Chem. **2006**, *45*, 10391−10402

Synthesis and Catalytic Epoxidation Activity with TBHP and H_2O_2 of Dioxo-, Oxoperoxo-, and Oxodiperoxo Molybdenum(VI) and Tungsten(VI) Compounds Containing Monodentate or Bidentate Phosphine Oxide Ligands: Crystal Structures of $WCl_2(O)_2(OPMePh_2)_2$, $WCl_2(O)(O_2)(OPMePh_2)_2$, $MoCl_2(O)_2dppmO_2 \cdot C_4H_{10}O$, $WCl_2(O)_2dppmO_2$, $Mo(O)(O_2)_2dppmO_2$, and $W(O)(O_2)_2dppmO_2$

Ampa Jimtaisong and Rudy L. Luck*

Department of Chemistry, Michigan Technological University, 1400 Townsend Drive, Houghton, Michigan 49931

Received August 2, 2006

The dioxo tungsten(VI) and molybdenum(VI) complexes $WCl_2(O)_2(OPMePh_2)_2$, $WCl_2(O)_2dppmO_2$, and $MoCl_2(O)_2$-$dppmO_2$, the oxoperoxo compounds $WCl_2(O)(O_2)(OPMePh_2)_2$, $WCl_2(O)(O_2)dppmO_2$, and $MoCl_2(O)(O_2)dppmO_2$, and the oxodiperoxo complexes, $W(O)(O_2)_2dppmO_2$ and $Mo(O)(O_2)_2dppmO_2$ have been prepared and characterized by IR spectroscopy, ^{31}P NMR spectroscopy, elemental analysis, and X-ray crystallography. The structural and X-ray crystallographic data of compounds $WCl_2(O)_2(OPMePh_2)_2$, $WCl_2(O)(O_2)(OPMePh_2)_2$, $MoCl_2(O)_2dppmO_2 \cdot C_4H_{10}O$, $WCl_2(O)_2dppmO_2$, $Mo(O)(O_2)_2dppmO_2$, and $W(O)(O_2)_2dppmO_2$ are also detailed. All complexes were studied as catalysts for *cis*-cyclooctene epoxidation in the presence of *tert*-butyl hydroperoxide (TBHP) or H_2O_2 as an oxidant. The Mo-based catalysts showed a superior reactivity over W-based catalysts in the TBHP system. On the other hand, in the H_2O_2 system, the W-based catalysts (accomplishing nearly 100% epoxidation of cyclooctene in 6 h) are more reactive than the Mo catalysts (<45% under some conditions). Various solvent systems have been investigated, and ethanol is the most suitable solvent for the H_2O_2 system.

1. Introduction

Olefin epoxidation is an important reaction in organic synthesis for the reason that epoxides are valuable and resourceful commercial intermediates, owing to the large range of reactions they undergo.[1] There are many ways available to accomplish olefin epoxidation. Those methods utilizing the peroxide moiety generally involve the addition of other reagents to activate the peroxide compound. Epoxidation of alkenes using peroxycarboxylic acids was detailed nearly a century ago.[2] More recently, metal-catalyzed epoxidation of olefins has been investigated, especially those systems that used organic peroxides combined with high-valence compounds such as Mo(VI), W(VI), and Re(VII) complexes.[3] It has been noted that the large positive charge of the metals make these compounds capable of accepting electron pairs in vacant d orbitals, resulting in stable complexes with organic peroxides. This formation causes the peroxidic distal oxygen atom to be more electrophilic and, therefore, more likely to be attacked by an olefinic double bond.[3a] Numerous studies have been conducted on metal-catalyzed epoxidation for both reactivity[3b,4] and mechanistic studies.[5,6] Dioxomolybdenum(VI) and dioxotungsten-

* To whom correspondence should be addressed. E-mail: rluck@mtu.edu.

(1) (a) Bhaduri, S.; Mukesh, D. *Homogeneous Catalysis: Mechanisms and Industrial Applications*; Wiley-Interscience: New York, 2000. (b) Cornils, B.; Herrmann W. A. Eds.; *Applied Homogeneous Catalysis with Organometallic Compounds*, 2nd ed.; Wiley-VCH: Weinheim, 2002; Vol. 1.

(2) (a) Prilezhaev, N. *Ber*. **1910**, *42*, 4811−4815. (b) Swern, D. *Organic Peroxide*; Wiley-Interscience, New York, 1971; Vol. 2.

(3) (a) Sheldon, R. A.; Van Doorn, J. A. *J. Catal*. **1973**, *31*, 427−437. (b) Jørgensen, K. A. *Chem. Rev*. **1989**, *89*, 431−458. (c) Kühn, F. E.; Santos, A. M.; Gonçalves, I. S.; Romão, C. C.; Lopes, A. D. *Appl. Organomet. Chem.* **2001**, *15*, 43−50. (d) Kühn, F. E.; Santos, A. M.; Abrantes, M. *Chem. Rev.* **2006**, *106*, 2455−2475. (e) Kühn, F. E.; Santos, A. M.; Herrmann, W. A. *Dalton Trans*. **2005**, 2483−2491.

(4) (a) Chaumette, P.; Mimoun, H.; Saussine, L.; Fischer, J.; Mitschler, A. *J. Organomet. Chem.* **1983**, *250*, 291−310. (b) Trost, M. K.; Bergman, R. G. *Organometallics* **1991**, *10*, 1172−1178. (c) Park, S.-W.; Kim, K.-J.; Seung, S. Y. *Bull. Korean Chem. Soc*. **2000**, *21*, 446−448. (d) Wang, Y.-L.; Ng, D. K. P.; Lee, H. K. *Inorg. Chem*. **2002**, *41*, 5276−5285.

10.1021/ic061455d CCC: $33.50
Published on Web 11/09/2006

(VI) compounds of general formulas $MX_2(O)_2(L)_2$ have been proven to be effective catalysts.[3c,7] For example, $MoBr_2(O)_2(NCR)_2$, R = CH_3 or C_6H_5, has been shown to accomplish the epoxidation of *cis*-cyclooctene in a 65% yield. However, these catalysts are not very stable and they decompose during the course of the reaction.[8] Bidentate and tridentate ligands bearing N-, O-, and S-electron donors are of interest and have been synthesized in order to stabilize the catalysts and improve the reactivity. For example, the complex dichlorodioxomolybdenum(VI) containing the 2,2-di(1-pyrazolyl)propane ligand has been reported.[9] This complex displayed a moderate catalytic reactivity (i.e., 65% cyclooctene epoxide after 4 h and 100% at 24 h reaction time). However, the stability of the catalyst was only slightly enhanced. Additionally, complexes of formulas $MoX_2(O)_2(L)_2$, where X = Cl, Br or Me and L_2 = 2,2′- bipyridine or 2,2′-bipyrimidine, have been established and appear to be stable catalysts. However, the catalytic reactivity can be considered as moderate, as these produced only 75% cyclooctene epoxide after 24 h.[10] Other activators, most recently, $NaHCO_3$ have been added to the catalytic mixture to activate hydrogen peroxide to effect the epoxidation.[11] The mechanism by which the oxygen atom (from a metal-bonded peroxo activated entity) is transferred to the olefin may be direct transfer.[12] Although the area of catalytic epoxide formation has been widely investigated judging from the literature, several fundamental problems still remain. A search for a procedure that would accomplish high yield and selectivity with a simple procedure, combining favorable economics and environmental concerns among other factors, is still a goal for industry.[13] This establishment of a more efficient and selective catalysts is an active area of research as many recently published studies attest.[14] Obviously, it would be reasonable to have an epoxidation reaction that involved only the catalyst, substrate, and H_2O_2,[15] and we are interested in designing such a catalyst. Clearly, if this direct oxygen transfer mechanism is operative, then the more activated the O atoms, the more facile is the transfer.

We have previously established that $MoCl_2(O)_2(OPMePh_2)_2$ (**1**) and $MoCl_2(O)(O_2)(OPMePh_2)_2$ (**2**) compounds can be used as catalysts for the isomerization of allylic alcohols and epoxidation of cyclohexene.[16] In this paper, the syntheses of compounds $WCl_2(O)_2(OPMePh_2)_2$ (**3**), $WCl_2(O)(O_2)(OPMePh_2)_2$ (**4**), $MoCl_2(O)_2dppmO_2$ (**5**), $MoCl_2(O)(O_2)dppmO_2$ (**6**), $WCl_2(O)_2dppmO_2$ (**7**), $WCl_2(O)(O_2)dppmO_2$ (**8**), $Mo(O)(O_2)_2dppmO_2$ (**9**), and $W(O)(O_2)_2dppmO_2$ (**10**) are reported. Compounds were synthesized and characterized using IR and NMR spectroscopic techniques, elemental analyses, and single-crystal X-ray crystallographic techniques. The catalytic epoxidation of *cis*-cyclooctene in the presence of either TBHP or H_2O_2 using the synthesized compounds as catalysts is detailed.

2. Experimental Section

2.1. General Method. Infrared spectra were obtained on a Mattson GL-3020 FTIR spectrometer. ^{31}P NMR data were recorded on a Varian XL-400 spectrometer. A Fisher-Johns melting point apparatus (Fisher Scientific Company) was used for the melting point determinations. The elemental analysis data were obtained from Galbraith Laboratories, Inc. A Shimadzu QP5050 GC-MS was used for the mass spectra determinations and quantitative analysis for the epoxidation reactions. Solvents were used as received from commercial suppliers. Most chemicals were purchased from Aldrich with the exception of methyl(diphenyl)phosphine oxide, which was purchased from either Aldrich or TCI America, and all chemicals were used as received. Bis(diphenylphosphineoxide)methane, $dppmO_2$, was prepared as described previously.[17] All compounds, except **4**, were recrystallized by being dissolved in CH_2Cl_2, stirred for about 1−2 h, concentrated and isolated by the addition of hexanes, and then vacuum-dried to obtain the reported yields and samples for elemental analyses. As evidence of bulk purity, copies of the ^1H NMR spectra in $CDCl_3$ of compounds **3**−**10** have been submitted as Supporting Information. They all indicate the presence of H_2O.

2.2. Synthesis. 2.2.1. Synthesis and Characterization of $WCl_2(O)_2(OPMePh_2)_2$ (3). Tungsten(VI) chloride (1.00 g) and methyl(diphenyl)phosphine oxide (1.08 g) were dissolved in 15 mL of CH_2Cl_2, together with 2 equiv of water. The resulting orange-yellow solution was stirred until a dark blue solution formed, which was then treated with a 140 μL of 30% H_2O_2 solution. The resulting light purple solution was stirred for about 1 h, and then the solvent was concentrated under vacuum. The desired compound was

(5) (a) Sharpless, K. B.; Townsend, J. M.; Williams, D. R. *J. Am. Chem. Soc.* **1972**, *94*, 295−296. (b) Thiel, W. R.; Priermeier, T. *Angew. Chem., Int. Ed. Engl.* **1995**, *34*, 1737−1738. (c) Mitchell, J. M.; Finney, N. S. *J. Am. Chem. Soc.* **2001**, *123*, 862−869. (d) Groarke, M.; Gonçalves, I. S.; Herrmann, W. A.; Kühn, F. E. *J. Organomet. Chem.* **2002**, *649*, 108−112.

(6) (a) Deubel, D. V.; Sundermeyer, J.; Frenking, G. *Inorg. Chem.* **2000**, *39*, 2314−2320. (b) Di Valentin, C.; Gisdakis, P.; Yudanov, I. V.; Rösch, N. *J. Org. Chem.* **2000**, *65*, 2996−3004. (c) Hroch, A.; Gemmecker, G.; Thiel, W. R. *Eur. J. Inorg. Chem.* **2000**, *5*, 1107−1114. (d) Deubel, D. V. *J. Phys. Chem. A.* **2001**, *105*, 4765−4772. (e) Gisdakis, P.; Yudanov, I. V.; Rösch, N. *Inorg. Chem.* **2001**, *40*, 3755−3765.

(7) Kühn, F. E.; Xue, W.-M.; Al-Ajlouni, A.; Santos, A. M.; Zang, S.; Romão, C. C.; Eickerling, G.; Herdtweck, E. *Inorg. Chem.* **2002**, *41*, 4468−4477.

(8) Kühn, F. E.; Herdtweck, E.; Haider, J. J.; Herrmann, W. A.; Gonçalves, I. S.; Lopes, A. D.; Romão, C. C. *J. Organomet. Chem.* **1999**, *583*, 3−10.

(9) Santos, A. M.; Kühn, F. E.; Bruus-Jensen, K.; Lucas, I.; Romão, C. C.; Herdtweck, E. *J. Chem. Soc., Dalton Trans.* **2001**, *8*, 1332−1337.

(10) (a) Kühn, F. E.; Groarke, M.; Bencze, É.; Herdtweck, E.; Prazeres, A.; Santos, A. M.; Calhorda, M. J.; Romão,C. C.; Gonçalves, I. S.; Lopes, A. D.; Pillinger, M. *Chem.—Eur. J.* **2002**, *8*, 2370−2383. (b) Veiros, L. F.; Prazeres, A.; Costa, P. J.; Romão, C. C.; Kühn, F. E.; Calhorda, M. J. *Dalton Trans.* **2006**, 1383−1389.

(11) (a) Lane, B. S.; Vogt, M.; DeRose, V. J.; Burgess, K. *J. Am. Chem. Soc.* **2002**, *124*, 11946−11954. (b) Gharah, N.; Chakraborty, S.; Mukherjee, A. K.; Bhattacharyya, R. *Chem. Commun.* **2004**, 2630−2632.

(12) Mitchell, J. M.; Finney, N. S. *J. Chem. Am. Soc.* **2001**, *123*, 862−869.

(13) Sato, K.; Aoki, M.; Ogawa, M.; Hashimoto, T.; Noyori, R. *J. Org. Chem.* **1996**, *61*, 8310−8311.

(14) (a) Valente, A. A.; Gonçalves, I. S.; Lopes, A. D.; Rodríguez-Borges, J. E.; Pillinger, M.; Romão, C. C.; Rocha, J.; García-Mera, X. *New J. Chem.* **2001**, *25*, 959−963. (b) Valente, A. A.; Moreira, J.; Lopes, A. D.; Pillinger, M.; Nunes, C. D.; Romão, C. C.; Kühn, F. E.; Gonçalves, I. S. *New J. Chem.* **2004**, *28*, 308−313. (c) Ambroziak, K.; Pelech, R.; Milchert, E.; Dziembowska, T.; Rozwadowski, Z. *J. Mol. Catal. A* **2004**, *211*, 9−16. (d) Valente, A. A.; Petrovski, Ž.; Branco, L. C.; Afonso, C. A. M.; Pillinger, M.; Lopes, A. D.; Romão, C. C.; Nunes, C. D.; Gonçalves, I. S. *J. Mol. Catal. A* **2004**, *218*, 5−11.

(15) Collins, T. J. *Acc. Chem. Res.* **2002**, *35*, 782−790.

(16) Fronczek, F. R.; Luck, R. L.; Wang, G. *Inorg. Chem. Commun.* **2002**, *5*, 384−387.

(17) White, C. R.; Joesten, M. D. *J. Inorg. Nucl. Chem.* **1967**, *38*, 2173-2175.

isolated by adding hexanes to the solution, and a light purple precipitate was filtered off, repurified as described above, and dried under vacuum yielding 1.73 g (96%) of compound **3**. Anal. Calcd for $C_{26}H_{26}Cl_2O_4P_2W$: C, 43.42; H, 3.64. Found: C, 42.97; H, 3.71%. mp 195−200 °C dec; ^{31}P NMR (CH_2Cl_2): δ 46.44 (s, 1P) relative to H_3PO_4. IR (Nujol mull, ν cm^{-1}) 1301s, 1152w, 1129s, 1081w, 996m, 956s (W═O), 911s (W═O), 895s, 778s, 753s, 724s, 718s, 690s.

2.2.2. Synthesis and Characterization of $WCl_2(O)(O_2)(OPMePh_2)_2$ (4). $WCl_2(O)_2(OPMePh_2)_2$ (1.00 g) was dissolved in 25 mL of CH_2Cl_2 and then treated with 1 equiv of 30% H_2O_2. The mixture was stirred for 5 h and then concentrated under vacuum. The desired compound was isolated and dried using a process similar to the one mentioned for the synthesis of **3**. The final product is a white powder obtained in 56% yield (0.57 g). Anal. Calcd for $C_{26}H_{26}Cl_2O_5P_2W\cdot H_2O$: C, 41.46; H, 3.75. Found: C, 41.19; H, 3.49%. mp 155−159 °C dec; ^{31}P NMR (CH_2Cl_2): δ 54.09 (s, 1P) and 46.06 (s, 1P) relative to H_3PO_4. IR (Nujol mull, ν cm^{-1}) 1302m, 1157m, 1130m, 1090m, 956s (W═O), 893s (O−O), 780m, 741m, 720m, 686m.

2.2.3. Synthesis and Characterization of $MoCl_2(O)_2dppmO_2$ (5). Lead molybdate (1.00 g) was moistened with CH_2Cl_2 (1.0 mL), and acetyl chloride (2.5 mL) was added. The resulting mixture was stirred for 30 min and then filtered. The residue was washed with a small amount of CH_2Cl_2. Addition of a $dppmO_2$ solution (1.14 g in 70 mL CH_2Cl_2) to a brown filtrate resulted in a brown solution and a yellow precipitate. This was stirred for 12 h, and the yellow precipitate was then filtered off, recrystallized, and dried under vacuum yielding 1.42 g (85%) of **5**. Anal. Calcd for $C_{25}H_{22}Cl_2O_4P_2Mo\cdot H_2O$: C, 47.42; H, 3.82. Found: C, 47.93; H, 3.66%. mp 295−300 °C dec; ^{31}P NMR (CH_2Cl_2): δ 38.39 (s, 1P) relative to H_3PO_4. IR (Nujol mull, ν cm^{-1}) 1264m, 1154s, 1123m, 1096m, 996m, 949s (M═O), 908s (M═O), 783s, 729s, 688s.

2.2.4. Synthesis and Characterization of $MoCl_2(O)(O_2)dppmO_2$ (6). $MoCl_2(O)_2dppmO_2$ (0.30 g) was dissolved in 70 mL of CH_2Cl_2, and 1 equiv of 30% H_2O_2 was added. The mixture was stirred for 1 day. The compound was obtained by concentrating the solution under vacuum, with hexanes added to effect precipitation followed by filtration. The filtered precipitate was recrystallized and dried at 60 °C under vacuum to yield 0.225 g (73%) yellow powder of **6**. Anal. Calcd for $C_{25}H_{22}Cl_2O_5P_2Mo$: C, 47.57; H, 3.51. Found: C, 48.08; H, 3.60%. mp 190−195 °C dec; ^{31}P NMR (CH_2Cl_2): δ 38.3 (d, 1P, J = 15.2 Hz) and 45.7 (d, 1P, J = 15.2 Hz) relative to H_3PO_4. IR (Nujol mull, ν cm^{-1}) 1148m, 1096m, 965s (M═O), 920s (O−O), 784s, 726s, 689s.

2.2.5. Synthesis and Characterization of $WCl_2(O)_2dppmO_2$ (7). Tungsten(VI) chloride (0.62 g) and $dppmO_2$ (0.65 g) were dissolved in 70 mL of CH_2Cl_2, followed by addition of 2 equiv of H_2O to the mixture. The resulting light green solution with a light green precipitate was stirred for 12 h, and the precipitate isolated by filtration. A light green precipitate was recrystallized and then dried under vacuum to yield 0.99 g (90%) of **7**. Anal. Calcd for $C_{25}H_{22}Cl_2O_4P_2W\cdot H_2O$: C, 41.64; H, 3.35. Found: C, 41.37; H, 3.20%. mp 285−290 °C dec; ^{31}P NMR (CH_2Cl_2) δ 39.58 (1s, P) relative to H_3PO_4. IR (Nujol mull, ν cm^{-1}) 1157s, 1125s, 1096s, 1026m, 996m, 963s (W═O), 943m, 913s (W═O), 889m, 785s, 738s, 690s.

2.2.6. Synthesis and Characterization of $WCl_2(O)(O_2)dppmO_2$ (8). $WCl_2(O)_2dppmO_2$ (0.20 g) was dissolved in 200 mL of CH_2Cl_2 followed by the addition of 87 μL of 30% H_2O_2. The resulting mixture was stirred for 1 day, and the product isolated and dried using the same procedure mentioned for the preparation of **6**. The desired compound was obtained as a white powder in 78% yield (0.16 g). Anal. Calcd for $C_{25}H_{22}Cl_2O_5P_2W$: C, 41.75; H, 3.08. Found: C, 41.60; H, 3.21%. mp 235−240 °C dec; ^{31}P NMR (CH_2Cl_2) δ 39.6 (d, 1P, J = 15.2 Hz) and 45.8 (d, 1P, J = 15.2 Hz) relative to H_3PO_4. IR (Nujol mull, ν cm^{-1}) 1147m, 1093m, 962s (M═O), 892s (O−O), 788s, 726s, 689s.

2.2.7. Synthesis and Characterization of $Mo(O)(O_2)_2dppmO_2$ (9). $MoCl_2(O)_2dppmO_2$ (0.20 g, 0.33 mmol) was dissolved in 150 mL of CH_2Cl_2 followed by the addition of 170 μL of 30% H_2O_2 (1.65 mmol). The mixture was stirred for 1 day, and the compound isolated and dried using a similar process to that used for **3**. The product had a yellow color and was obtained in a 79% yield (0.15 g). Anal. Calcd for $C_{25}H_{22}O_7P_2Mo\cdot 0.5H_2O$: C, 49.93; H, 3.86. Found: C, 49.80; H, 3.96%. mp 170−175 °C dec; ^{31}P NMR (CH_2Cl_2) δ 31.3 (br, 1P) and 49.3 (br, 1P) relative to H_3PO_4. IR (Nujol mull, ν cm^{-1}) 1169br, 1132br, 1084m, 1070m, 1056m, 961s, 953s, 875m, 867s, 786 s, 772m, 756m, 742s, 734m, 694s, 659s.

2.2.8. Synthesis and Characterization of $W(O)(O_2)_2dppmO_2$ (10). $WCl_2(O)_2dppmO_2$ (0.20 g, 0.28 mmol) was dissolved in 150 mL of CH_2Cl_2 followed by addition of 230 μL of 30% H_2O_2 (2.30 mmol). This mixture was stirred for 1 day, and the compound isolated and dried using a process similar to that mentioned for the synthesis of **3**. The final product is a white powder and was obtained in 84% yield (0.16 g). Anal. Calcd for $C_{25}H_{22}O_7P_2W\cdot H_2O$: C, 43.00; H, 3.46. Found: C, 42.41; H, 3.28%. mp 180−185 °C dec; ^{31}P NMR (CH_2Cl_2) δ 33.3 (d, 1P, J = 15.2 Hz) and 51.3 (d, 1P, J = 15.2 Hz) relative to H_3PO_4. IR (Nujol mull, ν cm^{-1}) 1157s, 1127m, 1097m, 1083m, 1069m, 1055 m, 995m, 966s, 958s, 851m, 840s, 787s, 773m, 743s, 694s, 650s.

2.3. Preparation of Single Crystals. Crystals were obtained using the solvent layering method. Typically, the compound was dissolved in a dense chlorinated solvent such as CH_2Cl_2 in a crystallizing tube, and then carefully a top layer was added with a less dense solvent such as hexane, ether, or toluene. This was sealed with Parafilm and left undisturbed at room temperature for about a week. The resulting slow diffusion of solvent across the boundary layer usually resulted in suitable crystals.

2.4. X-ray Crystallography. Suitable crystals were rolled in epoxy resin and mounted on glass fibers. An Enraf Nonius CAD-4 X-ray diffractometer was the instrument used in the measurements. The Windows program WinGX was used as the interface for the solution and refinement of the models.[18] The data were first reduced and corrected for absorption using ψ-scans[19] and then solved using the program SIR97.[20] The models were refined using the SHELXL97.[21]

Various types of disorder and decompositions features were evident in the structures. First, in compound **3**, one phenyl group was present in two orientations in a 62:38 occupancy ratio. Second, compound **4** contained unequal disorder between the terminal O and O_2 ligands in a 63:37 occupancy ratio. Compound **5** appeared to contain a disordered diethyl ether molecule of crystallization that was slowly evaporating out of the crystal lattice, as evident by the 44% decomposition in the intensity standards' reflections. The data for this compound was not as 'accurate' as that for the other structures reported, and interestingly enough, this situation pertained

(18) Farrugia, L. J. *J. Appl. Crystallogr.* **1999**, *32*, 837−838.
(19) North, A. C. T.; Phillips, D. C.; Mathews, F. S. *Acta Crystallogr. A.* **1968**, *24*, 351−359.
(20) Altomare, A.; Burla, M. C.; Camalli, M.; Cascarano, G.; Giacovazzo, C.; Guagliardi, A.; Moliterni, A. G. G.; Polidori, G.; Spagna, R. *J. Appl. Crystallogr.* **1999**, *32*, 115−119.
(21) Sheldrick, G. M. *SHELX-97. Programs for Crystal Structure Analysis (Release 97-2)*; University of Göttingen: Göttingen, Germany, 1998.

Scheme 1. Synthetic Pathways for Compounds **1**−**10**

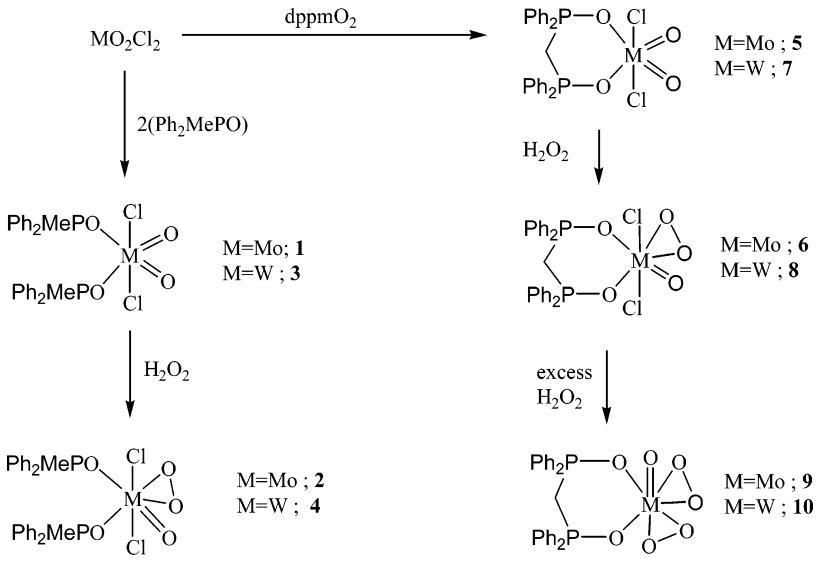

with data reported for an acetone solvate of **5**.[22] The refinement of complex **7** was straightforward, but complexes **9** and **10** both contained rotational disorder, essentially a 2-fold rotation about the $dppmO_2M$ (M = Mo, **9**; W, **10**) ligand to differing degrees. Compound **9** contained a 70:30 disorder, while that of **10** was 65:35.

2.5. Catalytic Reactions in the Presence of TBHP. The catalytic reactions were performed under an air atmosphere in a reaction vessel equipped with a magnetic stirrer and condenser. The reaction vessel was immersed into an oil bath, and 0.200 mg (1.8 mmol) of *cis*-cyclooctene, 1 mol % of catalyst (18 μmol), and 0.5 mL of 5.5 M TBHP were added to start the reaction. The mixture was heated at a specific temperature and reaction time. Samples were withdrawn periodically and analyzed using a Shimadzu QP5050 GC-MS. The products were quantified using calibration curves, and 200 mg of dibutyl ether was used as the internal standard (added after the reaction).

2.6. Catalytic Reactions in the Presence of H_2O_2. The catalytic reactions were performed under an air atmosphere using the same design as mentioned in the TBHP system. In a typical reaction, 0.200 mg (1.8 mmol) of *cis*-cyclooctene, 1 mol % catalyst (18 μmol) in 2 mL solvent, and 0.31 g of 30% H_2O_2 (1.5 equiv) were added to start the reaction. The reaction was then heated for a specific temperature and reaction time. Samples were analyzed using a Shimadzu QP5050 GC-MS. The products were quantified using calibration curves, and 200 mg of dibutyl ether (or decane) was used as an internal standard (added after the reaction).

3. Results and Discussion

3.1. Synthesis of Dioxo- and Oxoperoxo Mo(VI) and W(VI) Complexes. We have previously communicated the synthesis, spectroscopic properties, and some catalytic applications for compounds **1** and **2**.[16] We have now expanded our study to the dioxo and oxoperoxo W(VI) compounds. Additionally, dioxo and oxoperoxo complexes of $MoCl_2$(VI) and WCl_2(VI) with the bidentate ligand, $dppmO_2$, which may offer a more stable catalyst, were also synthesized.

W(VI) complexes of formula $WCl_2(O)_2(OPR_3)_2$ were reported for the first time by Brisdon in 1967.[23] However, the literature procedures for the synthesis of $WCl_2(O)_2(OPR_3)_2$, where R = (C_6H_5), reported a fairly low yield of the compound (27%). Herein, we report an alternative synthetic pathway for compounds with general formula $WCl_2(O)_2(OPR_3)_2$. This preparation consists of first dissolving WCl_6 and 2 equiv of the ligand in an appropriate amount of dichloromethane followed by treatment of this solution with 2 equiv of water. The solution is then stirred for an appropriate time resulting in the desired $WCl_2(O)_2(OPR_3)_2$ compounds. However, with the $OPMePh_2$ ligand, the resulting blue solution contained a mixture of the W(V) and W(VI) derivatives.[23] This mixture must be treated with an appropriate amount of H_2O_2 (0.5−1 mol equiv) to obtain a light purple-colored solution of the pure W(VI) compound (as confirmed by ^{31}P NMR data). Compound **3** was produced in a high yield (96%). Compound **7** was also synthesized using the same route in a 90% yield and without the addition of H_2O_2.

We have also discovered that the addition of 1 equiv of H_2O_2 to $MCl_2(O)_2(OPR_3)_2$, M = Mo or W; OPR_3 = monodentate or bidentate phosphine oxides, leads to the formation of the oxoperoxo complexes, $MCl_2(O)(O_2)(OPR_3)_2$. Additionally, the addition of an excess of H_2O_2 to the dioxo compounds bearing the $dppmO_2$ ligand resulted in the formation of the oxodiperoxo, $M(O)(O_2)_2dppmO_2$ compounds. The formation of compounds **1**−**10** is summarized in Scheme 1.

Strangely enough, complexes **3** and **4** are less soluble in organic solvents than their Mo(VI) analogues. Also those complexes containing the bidentate $dppmO_2$ ligand have reduced solubility compared to the other compounds. All compounds can be stored and handled under open atmospheric conditions without signs of decomposition. However, those complexes containing the peroxo ligand are less stable than their respective dioxo precursor compounds judging by the fact that they melt with decomposition at much lower temperatures (ca. >40 °C, see Experimental Section).

Interestingly, attempts to grow crystals of compounds **6** and **8** by several methods failed and resulted in the formation

(22) Hursthouse, M. B.; Levason, W.; Ratnani, R.; Reid, G. *Polyhedron* **2004**, *23*, 1915−1921.
(23) Brisdon, B. J. *Inorg. Chem.* **1967**, *10*, 1791−1795.

of the corresponding dioxo materials. We have studied the stability of the compounds using ^{31}P NMR monitoring and the results indicate that compounds **6** and **8** in CH_2Cl_2 solvent are stable (under NMR spectroscopic conditions). However, these oxoperoxo species readily transform back to the corresponding dioxo species in other solvents such as acetone or acetonitrile (shown in eq 1), as confirmed by ^{31}P NMR measurements.

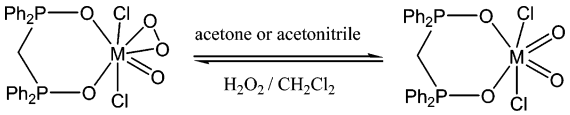

M=Mo, **6**
M=W, **8**

M=Mo, **5**
M=W, **7**

(**1**)

3.2. Spectroscopic Characterization. 3.2.1. IR Spectroscopic Data. The dioxomolybdenum(VI) compounds, **1** and **5**, showed two strong υ(M═O) absorption bands in the 908−903 and 949−942 cm^{-1} regions. The corresponding dioxotungsten (VI) compounds, **3** and **7**, contained the υ(W═O) absorption bands in the 913−911 and 963−956 cm^{-1} regions. These absorptions are assigned to the asymmetric and symmetric stretching modes for the cis dioxo unit, and they are in the expected range.[4d,23,24] The υ(P═O) stretching band of free $OPMePh_2$ is at 1171 cm^{-1} and this shifts to the 1155−1152 cm^{-1} region in the compounds. In the $dppmO_2$ compounds (**5**−**10**), the P═O band shifts from 1189 cm^{-1} in the free ligand to the 1157−1147 cm^{-1} region.

The oxoperoxomolybdenum(VI) compounds, **2** and **6**, displayed υ(Mo═O) bands in the 965−956 cm^{-1} region and the absorbance for the υ(O−O) stretching mode is at 920 cm^{-1}. The oxoperoxotungsten(VI) complexes, **4** and **8**, contained a band in the 964−956 cm^{-1} region which is assigned to the υ(W═O) stretching mode, and another band at about 892 cm^{-1} was also observed and tentatively assigned as the υ(O−O) stretching mode. The υ(P═O) bands in these compound are observed in the 1157−1152 cm^{-1} region for compounds **2** and **4** and at about 1147 cm^{-1} for compounds **6** and **8**.

The oxodiperoxo complexes, $M(O)(O_2)_2dppmO_2$, **9** and **10**, contain strong absorption bands at 961, 953 and 966, 958 cm^{-1} for the Mo and W complexes, respectively. Additional bands at 875, 864 and 851, 840 cm^{-1} are also observed and tentatively assigned for the υ(O−O) stretching absorptions for the Mo (**9**) and W (**10**), complexes, respectively. Selected IR spectroscopic data for compounds **1**−**10** together with assignments are summarized in Table 1.

3.2.2. ^{31}P NMR Spectroscopic Data. ^{31}P NMR spectroscopy was used to determine the complexity of reaction mixtures or the purity of compounds containing phosphine oxide ligands.[25] The P atom in free $OPMePh_2$ resonates at 30 ppm relative to H_3PO_4. This shifts downfield to 44 and 46 ppm upon coordination via the oxygen atom to the metals in the dioxo Mo(VI) (**1**) and W(VI) (**3**), respectively. A single resonance suggests two equivalent phosphorus atoms in these compounds. For the oxoperoxo $MCl_2(O)(O_2)(OPMePh_2)_2$ complexes, the ^{31}P NMR spectra contained two resonances at 53 and 44 ppm for the Mo(VI) (**2**) and at 54 and 46 ppm for the W(VI) (**4**), respectively. The more downfield resonance in both cases can be assigned to the ligand trans to the peroxo group, while the more upfield may be assigned to the P atom in the ligand trans to the oxo-group on the basis of data from the dioxo complexes presented earlier.

The ^{31}P NMR spectra for $MCl_2(O)_2dppmO_2$ compounds, **5** and **7**, contained a single resonance at 38 and 39 ppm for the Mo(VI) and W(VI) complexes, respectively. The ^{31}P NMR spectrum in the oxoperxo $MCl_2(O)(O_2)dppmO_2$ compounds, **6** and **8**, consisted of two doublets indicating coupling between two nonequivalent phosphorus atoms, see Table 2.

Interestingly, the ^{31}P NMR spectra for **10** contained two doublet absorptions which indicated two nonequivalent phosphorus atoms in the compound. In contrast, the spectrum for compound **9** consisted of two broad peaks under the same conditions (i.e., 25 °C). This spectrum still contained two broad peaks at 35 °C but at reduced intensity. Further study at higher temperatures was limited by the low solubility of compound **9** in higher-boiling-point solvents. However, a low temperature ^{31}P NMR study of **9** showed that, at 10 and 0 °C, two single sharp peaks are observed and, at −10 and

Table 1. Selected Wavenumbers (cm^{-1}) for the M═O and O−O Stretching Modes for **1**−**10**[a]

compound	M═O	M═O asym
$MoCl_2(O)_2(OPMePh_2)_2$ (**1**)	942s	903s
$MoCl_2(O)_2dppmO_2$ (**5**)	949s	908s
$WCl_2(O)_2(OPMePh_2)_2$ (**3**)	956s	911s
$WCl_2(O)_2dppmO_2$ (**7**)	963s	913s
	M═O	O−O
$MoCl_2(O)(O_2)(OPMePh_2)_2$ (**2**)	956s	920s
$MoCl_2(O)(O_2)dppmO_2$ (**6**)	965s	920s
$WCl_2(O)(O_2)(OPMePh_2)_2$ (**4**)	956s	893s
$WCl_2(O)(O_2)dppmO_2$ (**8**)	963s	892s
$Mo(O)(O_2)_2dppmO_2$ (**9**)	961s, 953s (d)	875w, 864s
$W(O)(O_2)_2dppmO_2$ (**10**)	966s, 958s (d)	851w, 840s

[a] s = strong, w = weak, (d) = doublet.

Table 2. ^{31}P NMR Chemical Shift of the Free Ligands and the Compounds **1**−**10** at 25 °C[a]

compound	^{31}P NMR (ppm)[b]
$OPMePh_2$	30.0 (s)
$dppmO_2$	23.0 (s)
$MoCl_2(O)_2(OPMePh_2)_2$ **1**	44.4 (s)
$MoCl_2(O)(O_2)(OPMePh_2)_2$ **2**	53.4 (s), 43.8 (s)
$WCl_2(O)_2(OPMePh_2)_2$ **3**	46.4 (s)
$WCl_2(O)(O_2)(OPMePh_2)_2$ **4**	54.1 (s), 46.1 (s)
$MoCl_2(O)_2dppmO_2$ **5**	38.4 (s)
$MoCl_2(O)(O_2)dppmO_2$ **6**	45.7 (d), 38.3 (d), J_{P-P} = 15.2 Hz
$WCl_2(O)_2dppmO_2$ **7**	39.6 (s)
$WCl_2(O)(O_2)dppmO_2$ **8**	45.8 (d), 39.6 (d), J_{P-P} = 15.2 Hz
$Mo(O)(O_2)_2dppmO_2$ **9**	49.3 (br, s), 31.3 (br, s)
$W(O)(O_2)_2dppmO_2$ **10**	51.3 (d), 33.3 (d), J_{P-P} = 15.2 Hz

[a] Compound was dissolved in CH_2Cl_2, and the H_3PO_4/D_2O in a sealed capillary was used as the internal reference. [b] s = singlet, d = doublet, br = broad.

(24) Butcher, R. J.; Gunz, H. P.; Maclagan, G. A. R.; Kipton, H.; Powell, J.; Wilkins, C.; Hian, Y. S. *J. Chem. Soc., Dalton Trans.* **1975**, *12*, 1223−1227.
(25) Garrou, P. E. *Chem. Rev.* **1981**, *81*, 229−266.

Table 3. Crystallographic Data for the Structures Provided

	3	**4**	**5**
formula	$C_{26}H_{26}Cl_2O_4P_2W$	$C_{26}H_{26}Cl_2O_5P_2W$	$C_{25}H_{22}Cl_2O_4P_2Mo.C_4H_{10}O$
fw, g·mol^{-1}	719.16	735.16	689.33
cryst syst	monoclinic	monoclinic	monoclinic
space group	*P*21/*c*	*P*21/*n*	*P*121/*n*1
a (Å)	9.225(2)	9.322(3)	11.141(2)
b (Å)	17.629(5)	17.429(4)	14.410(3)
c (Å)	17.867(3)	17.879(5)	18.474(4)
α (deg)	90	90	90
β (deg)	104.52(2)	105.17(3)	92.761(17)
γ (deg)	90	90	90
V (Å^3)	2812.9(11)	2803.6(14)	2962.4(11)
Z	4	4	4
d_{calcd} (g·cm^{-3})	1.698	1.742	1.546
μ (mm^{-1})	4.440	4.459	0.942
θ (deg)	1.65−22.49	1.66−22.48	1.79−22.52
λ (Å)	0.71073	0.71073	0.71073
T (K)	293(2)	293(2)	293(2)
GOF	1.032	1.099	1.046
R1[a], wR2 ($I > 2\sigma(I)$)[b]	0.033, 0.069[c]	0.057, 0.131[d]	0.087, 0.230 [e]
	7	**9**	**10**
formula	$C_{25}H_{22}Cl_2O_4P_2W$	$C_{25}H_{22}O_7P_2Mo$	$C_{25}H_{22}O_7P_2W$
fw, g·mol^{-1}	703.12	592.31	680.22
cryst syst	tetragonal	monoclinic	monoclinic
space group	I 41	P 21/n	P 21/n
a (Å)	19.268(2)	13.519(2)	13.479(3)
b (Å)	19.268(4)	10.978(3)	10.990(2)
c (Å)	28.587(4)	17.159(3)	17.278(5)
α (deg)	90	90	90
β (deg)	90	96.300(10)	96.44(2)
γ (deg)	90	90	90
V (Å^3)	10613(3)	2531.2(9)	2543.3(10)
Z	4	4	4
d_{calcd} (g·cm^{-3})	1.76	1.554	1.776
μ (mm^{-1})	4.705	0.687	4.710
θ (deg)	1.27−22.47	1.82−24.63	1.82−22.49
λ (Å)	0.71073	0.71073	0.71073
T (K)	293(2)	293(2)	293(2)
GOF	1.028	1.116	1.120
R1[a], wR2 ($I > 2\sigma(I)$)[b]	0.038, 0.092 [f]	0.067, 0.131 [g]	0.060, 0.094 [h]

[a] $R1 = \sum||F_o| - |F_c||/\sum|F_o|$. [b] $wR2 = [\sum[w(F_o^2 - F_c^2)^2]/\sum[w(F_o^2)^2]]^{1/2}$. [c] $w = 1/[^2(F_o^2) + (0.0330P)^2 + 4.0652P]$ where $P = (F_o^2 + 2(F_c)^2)/3$. [d] $w = 1/[^2(F_o^2) + (0.0840P)^2 + 7.2653P]$. [e] $w = 1/[^2(F_o^2) + (0.1600P)^2 + 20.6394P]$. [f] $w = 1/[^2(F_o^2) + (0.0622P)^2 + 0.0000P]$. [g] $w = 1/[^2(F_o^2) + (0.0000P)^2 + 23.6769P]$. [h] $w = 1/[^2(F_o^2) + (0.0000P)^2 + 23.3805P]$.

−20 °C, these resolve into two doublets. The ^{31}P NMR spectral shifts for compounds **1**−**10** are presented in Table 2.

3.3. X-ray Crystallographic Data. Crystals were obtained as described in the Experimental Section except for **9** which was achieved by allowing slow evaporation of an ethanol solution of **9**. Crystal data and final structural refinement parameters of all compounds are listed in Table 3.

3.3.1. Crystal Structure of 3. An ORTEP-3 [26] drawing of **3** is shown as Figure 1. The bond lengths and bond angles about the W atom are listed in Table 4. The coordination geometry about the W atom is a distorted octahedron in which two Cl atoms are axially trans (Cl1−W1−Cl2 angle = 165.07(8) °) and two oxo-oxygen atoms (O_{oxo}) are cis to each other and trans to the oxygen of the phosphine oxide ligands (O_{lig}), all located in a distorted equatorial plane. The bond distances for W═O_{oxo} and W−Cl are within the expected ranges of 1.70−1.75 and 2.34−2.39 Å, respectively.[7,27] The $OPMePh_2$ ligands are oriented in a cis configuration with an O11−W1−O21 angle of 77.44(19)°.

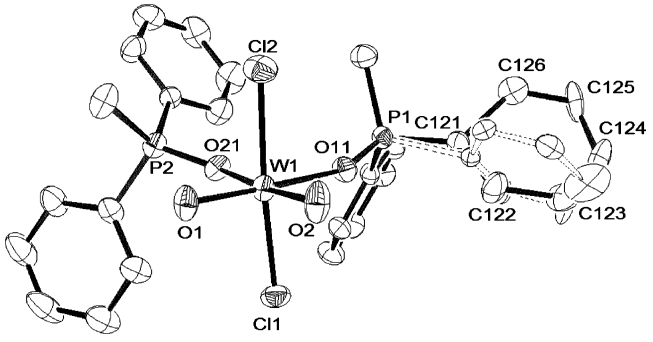

Figure 1. Crystal representation (ORTEP-3[26]) of **3** with selected atom numbering. Thermal ellipsoids are drawn at the 20% probability level, and hydrogen atoms are omitted for clarity. The major orientation in the disordered phenyl ring (62%, C121, C122, C123, C124, C125, and C126) on the right of the drawing is the one drawn with solid lines for the bonds. The minor phenyl ring is shown with dashed lines for the bonds.

The P−O bond distances and P−O−W angles, P1−O11 = 1.497(5) Å and P2−O21 = 1.523 (3) Å and P1−O11−W1 = 159.0(3)° and P2−O21−W1 = 139.5(3)°, are significantly different though in the range for coordinated phosphine oxides.[27a,28,29] These two molecules, i.e., complexes **1**[29] and **3**, are isostructural. Interestingly, one of the

(26) Farrugia, L. J. *J. Appl. Crystallogr.* **1997**, *30*, 565.

Table 4. Selected Bond Distances (Å) and Angles (deg) of **3**

W1−O1	1.706(5)	W1−O11	2.150(5)	W1−Cl1	2.386(2)	P1−O11	1.497(5)
W1−O2	1.716(5)	W1 O21	2.182(5)	W1−Cl2	2.388(2)	P2−O21	1.523(5)
O1−W1−O2	101.3(3)	O2−W1−O11	91.7(2)	O1−W1−Cl2	95.7(2)	O21−W1−Cl2	84.14(14)
O11−W1−O21	77.44(19)	O1−W1−O21	89.5(2)	O2−W1−Cl2	94.6(3)	Cl1−W1−Cl2	165.07(8)
O1−W1−O11	166.8(2)	O1−W1−Cl1	94.4(2)	O11−W1−Cl1	82.59(15)	P1−O11−W1	159.0(3)
O2−W1−O21	169.2(2)	O2−W1−Cl1	94.2(3)	O21−W1−Cl1	84.96(14)	P2−O21−W1	139.5(3)
				O11−W1−Cl2	85.10(14)		

Table 5. Selected Bond Distances (Å) and Angles (deg) for **4** (63% O1, O2, O3:37% O4, O5, O6 disordered)

W1−O1	1.85(2)	W1−O5	1.69(4)	O4−O5	1.52(5)	W1−Cl2	2.396(4)
W1−O2	1.846(18)	W1−O6	1.86(2)	W1−O11	2.093(8)	O11−P1	1.517(9)
W1−O3	1.739(14)	O1−O2	1.55(3)	W1−O21	2.098(8)	O21−P2	1.508(8)
W1−O4	1.79(2)			W1−Cl1	2.400(4)		
O2−W1−O3	105.6(8)	O2−W1−Cl1	73.5(7)	O5−W1−O4	51.5(18)	O6−W1−Cl2	95.1(9)
O3−W1−O11	87.9(5)	O3−W1−Cl2	90.8(7)	O4−W1−O6	96.0(9)	O5−W1−Cl1	123.8(17)
O1−W1−O11	153.3(8)	O1−W1−Cl2	72.4(7)	O5−W1−O6	95.8(15)	O4−W1−Cl1	73.3(8)
O2−W1−O11	152.5(7)	O2−W1−Cl2	121.0(7)	O6−W1−O21	90.6(7)	O6−W1−Cl1	100.3(9)
O1−W1−O21	90.3(7)	O1−W1−O2	49.5(9)	O4−W1−O21	157.9(8)	O11−W1 Cl1	80.9(3)
O2−W1−O21	88.0(6)	O1−W1−O3	98.8(8)	O5−W1−O21	148.7(17)	O11−W1−Cl2	81.7(3)
O3−W1−O21	166.4(6)	O11−W1−O21	79.5(3)	O4−W1−O11	93.9(7)	O21−W1−Cl1	84.7(3)
O3−W1−Cl1	98.5(7)	P1−O11−W1	140.1(5)	O5−W1−O11	91.7(14)	O21−W1−Cl2	82.3(3)
O1−W1−Cl1	123.0(8)	P2−O21−W1	162.1(6)	O6−W1−O11	169.9(7)	C12−W1−C11	159.93(17)

phenyl rings of the phosphine oxides exhibited a positional disorder where the minor orientation (38%) has an orientation roughly perpendicular to the major arrangement (62%). This type of disorder has also been observed for the Mo analogue,[29] and in both cases, the disorder occurred in the phosphine oxide ligand that had the larger P−O−M angle. Similar P−O−M angles have also been previously observed in other phosphine oxide coordination compounds.[28b,29] The corresponding $M-O_{lig}$ bond distances are significantly different in these reported compounds, i.e., $MoCl_3O(OPPh_3)_2$ 2.065(10) and 2.136(11) Å (ordered molecule)[28b] and $MoCl_2(O)_2(OPMePh_2)_2$ 2.160(3) and 2.206(3) Å.[29] Clearly, the more linear the P−O−M interaction, the greater the degree of bonding between the O and M atoms, as indicated by the shorter distances. However, in compound **3**, the $W-O_{lig}$ distances while significantly different, i.e., 2.150(5) and 2.182(5) Å, are closer to each other than those reported in the complexes mentioned above.

3.3.2. Crystal Structure of 4. An ORTEP-3 [26] representation of **4** is shown in Figure 2. Selected bond lengths and angles about the W atom are listed in Table 5. The compound crystallized with seven atoms coordinating around the W atom. The molecule contained a 63:37 disorder ratio between the peroxo and oxo ligands. The Cl ligands are oriented trans to each other with similar bond distances of 2.396(4) and 2.400(4) Å to various dichloro W species[7,27a,c,30] and a Cl1−W1−Cl2 angle of 159.93(17)°. The $OPMePh_2$ ligands are cis to each other and trans to the (disordered) oxo and peroxo ligands.

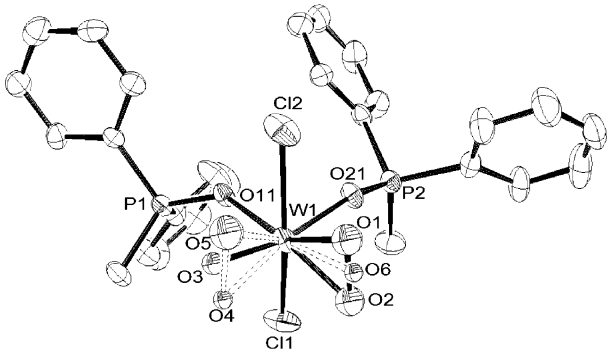

Figure 2. Crystal representation (ORTEP-3[26]) of **4** with selected atom numbering. Thermal ellipsoids are drawn at the 20% probability level. Hydrogen atoms are omitted for clarity. The crystal contained an oxo-, peroxo-ligand positional disorder with a 63% major orientation (O1−O2, and O3) and 37% (O4−O5 and O6) shown with dashed lines for the bonds.

The metal-to-disordered oxo-oxygen bond distances, W1−O3 1.739(14) and W1−O6 1.86(2) Å, are longer than the reported monooxo−tungsten bond distance range of 1.69−1.71 Å[27d,31] and those in **3** of 1.706(5) and 1.716(5) Å, and the $W-O_{peroxo}$ distances (1.69(4)−1.85(2) Å) are shorter than the reported values of 1.85−1.95 Å.[31] These differences probably are a result of the disorder between the oxo and peroxo ligands. Moreover, this disorder may have affected the trans effect of the oxo and peroxo ligands as can be seen from the similar W1−O11 and W1−O21 distances of 2.093(8) and 2.098(8) Å, respectively. The two W−O−P bond angles, 140.1(5)° and 162.1(6)°, are very different with no simple relationship to these similar bond lengths. Given the fact that a significant difference was also observed in the related angles in complex **3**, these angles may well result from steric considerations, i.e., packing effects.

3.3.3. Crystal Structure of 5. This crystal contains a disordered diethyl ether molecule of crystallization that was slowly evaporating out of the crystal lattice, as evident by

(27) (a) De Wet, J. F.; Caira, M. R.; Gellatly, B. J. *Acta Crystallogr. B* **1978**, *34*, 762−766. (b) Dreisch, K.; Andersson, C.; Håkansson, M.; Jagner, S. *J. Chem. Soc., Dalton Trans.* **1993**, *7*, 1045−1049. (c) Dreisch, K.; Andersson, C.; Stålhandske, C. *Polyhedron* **1991**, *10*, 2417−2421. (d) Mayer, J. M. *Inorg. Chem.* **1988**, *27*, 3899−3903.
(28) (a) Butcher, R. J.; Penfold, B. R.; Sinn, E. *J. Chem. Soc., Dalton Trans.* **1979**, 668−675. (b) Garner, C. D.; Howlader, N. C.; Mabbs, F. E.; McPhail, A. T.; Onan, K. D. *J. Chem. Soc., Dalton Trans.* **1978**, 1848−1854. (c) Wang, G.; Jimtaisong, A.; Luck, R. L. *Inorg. Chim. Acta* **2005**, *358*, 933−940.
(29) Fronczek, F. R.; Luck, R. L.; Wang, G. *Inorg. Chim. Acta* **2003**, *342C*, 247−254.
(30) Brock, S. L.; Mayer, J. M. *Inorg. Chem*. **1991**, *30*, 2138−2143.
(31) (a) Maiti, S. K.; Banerjee, S.; Mukherjee, A. K.; Abdul Malik, K. M.; Bhattacharyya, R. *New J. Chem.* **2005**, *29*, 554−563. (b) Piquemal, J.-Y.; Halut, S.; Brégeault, J.-M. *Angew. Chem., Int. Ed.* **1998**, *37*, 1146−1149. (c) Griffith, W. P.; Slawin, A. M. Z.; Thomson, K. M.; Williams, D. J. *J. Chem. Soc., Chem. Commun.* **1994**, 569−570.

Table 6. Selected Bond Distances (Å) and Angles (deg) for **5**

Mo1−O1	1.706(7)	Mo1−O11	2.177(6)	Mo1−Cl1	2.396(3)	P1−O11	1.511(6)
Mo1−O2	1.695(7)	Mo1−O21	2.208(6)	Mo1−Cl2	2.366(3)	P2−O21	1.505(7)
O1−Mo1−O2	103.5(4)	O1−Mo1−O11	88.1(3)	O11−Mo1−Cl2	85.13(18)	O21−Mo1−Cl1	83.45(18)
O11−Mo1−O21	78.5(2)	O2−Mo1−O21	89.8(3)	O21−Mo1−Cl2	82.71(19)	Cl2−Mo1−Cl1	163.15(11)
O2−Mo1−O11	168.0(3)	O2−Mo1−Cl2	96.5(4)	O2−Mo1−Cl1	93.0(4)	P1−O11−Mo1	142.2(3)
O1−Mo1−O21	166.6(3)	O1−Mo1−Cl2	95.6(3)	O1−Mo1−Cl1	95.6(3)	P2−O21−Mo1	140.7(4)
				O11−Mo1−Cl1	82.73(17)		

the 44% decrease of intensity for the data. As a result, the data for this compound were poor compared to that of the other structures reported (and this resulted in the high *R* factor values listed in Table 3). Interesting enough, similarly weak diffracting data for $MoCl_2(O)_2dppmO_2 \cdot 1/2CH_3C(O)CH_3$ was also reported.[22] The molecule consists of a distorted octahedral geometry about the Mo atom, as expected for an $MCl_2(O)_2L_2$ type compound, Figure 3. The two Cl atoms are oriented trans to each other with a Cl1−Mo1−Cl2 angle of 163.15(11)°, see Table 6. The two oxo ligands are cis to each other ($Mo-O_{avg} = 1.701(6)$ Å) and trans to the oxygen atoms of the $dppmO_2$ ligand. Interestingly, the P−O−Mo angles of 140.7(4)° and 142.4(3)° are not as different (diff. = 1.5°) compared to those in complex **3** (19.5°) and **4** (22°) containing monodentate phosphine oxide ligands.

3.3.4. Crystal Structure of 7. Compound **7** crystallized with two independent molecules constituting the asymmetric unit. An ORTEP-3[26] drawing of the molecules is given in Figure 4. As with most of the characterized dioxo compounds of formulas $MX_2(O)_2L_2$, M = Mo or W, X= halide, L = Lewis base ligand, the coordination geometry around the W center can be described as a distorted octahedron.[7,27,28a,32]

The overall arrangement of the six coordinating ligands around the W atom is similar to that in **5** and the Mo

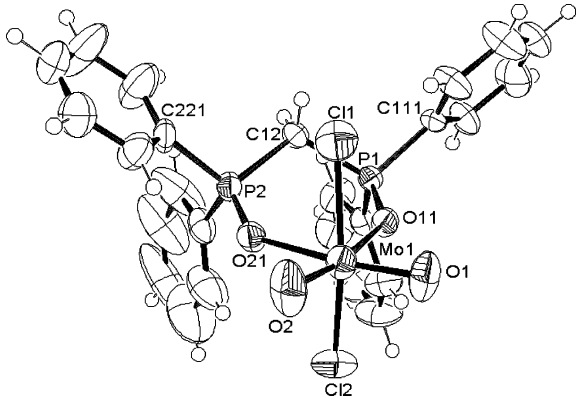

Figure 3. Crystal representation (ORTEP-3[26]) of **5** with selected atom numbering. Thermal ellipsoids are drawn at the 50% probability level. H atoms are represented by circles of arbitrary sized radii. The $C_4H_{10}O$ molecule of solvation is not shown.

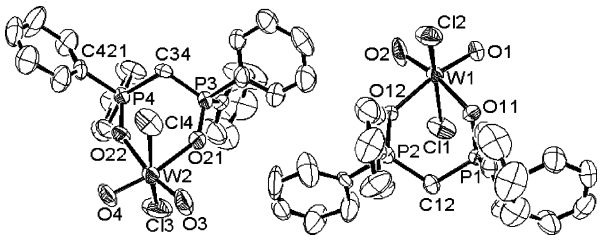

Figure 4. Crystal representation (ORTEP-3[26]) of the two independent molecules in **7** with selected atom numbering. Thermal ellipsoids are drawn at the 50% probability level. Hydrogen atoms are omitted for clarity.

Table 7. Selected Bond Distances (Å) and Angles (deg) for **7**

molecule 1		molecule 2	
W1−O1	1.726(10)	W2−O3	1.705(10)
W1−O2	1.693(10)	W2−O4	1.708(11)
W1−O11	2.184(9)	W2−O21	2.180(11)
W1−O12	2.180(10)	W2−O22	2.154(9)
W1−Cl1	2.398(4)	W2−Cl3	2.354(5)
W1−Cl2	2.359(4)	W2−Cl4	2.406(5)
P1−O11	1.505(10)	P3−O21	1.519(12)
P2−O12	1.517(11)	P4−O22	1.496(10)
O1−W1−O2	101.0(5)	O3−W2−O4	101.9(6)
O1−W1−O11	91.1(4)	O3−W2−O21	90.3(5)
O1−W1−O12	168.9(4)	O3−W2−O22	168.4(5)
O2−W1−O11	167.8(5)	O4−W2−O21	167.6(4)
O2−W1−O12	89.9(4)	O4−W2−O22	89.6(4)
O11−W1−O12	77.9(3)	O21−W2−O22	78.2(4)
O1−W1−Cl2	95.4(4)	O3−W2−Cl4	94.3(5)
O2−W1−Cl2	96.5(5)	O4−W2−Cl4	95.4(5)
O11−W1−Cl2	82.8(3)	O21−W2−Cl4	81.4(3)
O12−W1−Cl2	85.1(3)	O22−W2−Cl4	83.2(3)
O1−W1−Cl1	93.9(3)	O3−W2−Cl3	96.9(5)
O2−W1−Cl1	95.8(5)	O4−W2−Cl3	96.3(5)
O11−W1−Cl1	82.7(3)	O21−W2−Cl3	84.2(3)
O12−W1−Cl1	83.0(3)	O22−W2−Cl3	83.0(3)
Cl2−W1−Cl1	162.85(17)	Cl4−W2−Cl3	161.79(19)
P1−O11−W1	139.9(6)	P3−O21−W2	140.5(6)
P2−O12−W1	139.5(5)	P4−O22−W2	144.5(6)

analogue containing a different molecule of solvation,[22] i.e., the octahedron consists of cis dioxo, O1−W1−O2 (or O3−W2−O4) groups, trans dichloride ligands, and two neutral oxygen donors from the $dppmO_2$ ligand, both neutral oxygen trans to the cis dioxo group. The bond lengths and angles between the two molecules in **7**, see Table 7, do not vary significantly and are comparable to those observed in other dioxotungsten compounds.[7,27,32,33]

3.3.5. Crystal Structure of 9. Compound **9** has seven atoms coordinating around the Mo atom and also contained disorder with the oxygen atoms of the two peroxo and oxo ligands, as shown in Figure 5. The coordination geometry around the Mo center can be described as a distorted pentagonal bipyramid. With this assignment, the apical positions are occupied by the oxo oxygen; O1 (or O10) and one of the oxygen of the $dppmO_2$ ligand, i.e., O21 (or O11). The oxygen atoms from the peroxo groups, i.e., O2 and O3, O4, and O5 (or O2 and O30, O4, and O50), and the oxygen atoms from the $dppmO_2$ ligand, i.e., O21 (or O11) are situated in an equatorial plane. Selected bond parameters are listed in Table 8. The disorder in the arrangement of the

(32) (a) Spivack, B.; Dori, Z. *Coord. Chem. Rev.* **1975**, *17*, 99−136. (b) Wang, G.; Chen, G.; Luck, R. L.; Wang, Z.; Mu, Z.; Evans, D. G.; Duan, X. *Inorg. Chim. Acta* **2004**, *357*, 3223−3229. (c) Hornung, F. M.; Heilmann, O.; Kaim, W.; Zalis, S.; Fiedler, J. *Inorg. Chem.* **2000**, *39*, 4052−4058.

(33) (a) Zhang, C.; Schlemper, E. O.; Schrauzer, G. N. *Organometallics* **1990**, *9*, 1016−1020. (b) Wong, Y.-L.; Yan, Y.; Chan, E. S. H.; Yang, Q.; Mak, T. C. W.; Ng, D. K. P. *J. Chem. Soc., Dalton Trans.* **1998**, 3057−3064.

Table 8. Selected Bond Distances (Å) and Angles (deg) for **9** (70% O1, O3, O5:30% O10, O30, O50)

Mo1−O1	1.804(11)	Mo1−O30	1.63(2)	O2−O30	1.58(3)	Mo1−O11	2.240(6)
Mo1−O3	1.813(9)	Mo1−O50	1.78(2)	O4−O50	1.34(3)	Mo1−O21	2.133(7)
Mo1−O5	1.802(12)	O2−O3	1.404(13)	Mo1−O2	1.894(8)	O11−P1	1.503(6)
Mo1−O10	2.13(2)	O4−O5	1.420(14)	Mo1−O4	1.962(7)	O21−P2	1.502(7)
O1−Mo1−O2	95.8(5)	O3−Mo1−O4	138.5(5)	O10−Mo1−O4	87.7(7)	O30−Mo1−O50	103.2(14)
O1−Mo1−O4	99.7(5)	O3−Mo1−O5	96.3(6)	O10−Mo1−O2	92.6(7)	O50−Mo1−O2	155.8(9)
O1−Mo1−O3	101.2(5)	O3−Mo1−O11	87.3(4)	O10−Mo1−O30	96.0(12)	O50−Mo1−O4	41.7(9)
O1−Mo1−O5	102.3(6)	O3−Mo1−O21	132.5(5)	O10−Mo1−O50	90.7(12)	O50−Mo1−O11	122.9(9)
O1−Mo1−O11	164.3(4)	O4−Mo1−O5	44.1(4)	O10−Mo1−O21	156.8(7)	O50−Mo1−O21	98.0(10)
O1−Mo1−O21	84.8(4)	O4−Mo1−O11	81.8(3)	O10−Mo1−O11	77.5(7)	O11−Mo1−O21	79.7(2)
O2−Mo1−O3	44.5(4)	O4−Mo1−O21	84.7(3)	O30−Mo1−O2	52.6(11)	P1−O11−Mo1	132.0(4)
O2−Mo1−O5	139.7(5)	O5−Mo1−O11	89.6(4)	O30−Mo1−O4	144.9(11)	P2−O21−Mo1	136.4(4)
O2−Mo1−O11	81.1(3)	O5−Mo1−O21	128.8(4)	O30−Mo1−O11	133.2(11)	O2−Mo1−O4	162.4(3)
O2−Mo1−O21	88.2(3)			O30−Mo1−O21	102.8(11)		

molecules in the crystal lattice has drastically altered the resulting bond lengths in the molecule. The molybdenum to the oxo-oxygen distances, i.e., Mo1−O1 1.804(11) Å and Mo1−O10 2.13(2) Å) are significantly longer than the 1.65−1.69 Å range for the completely ordered oxodiperoxo compounds.[31a,32b,34] Most of the Mo−O_{peroxo} bond distances

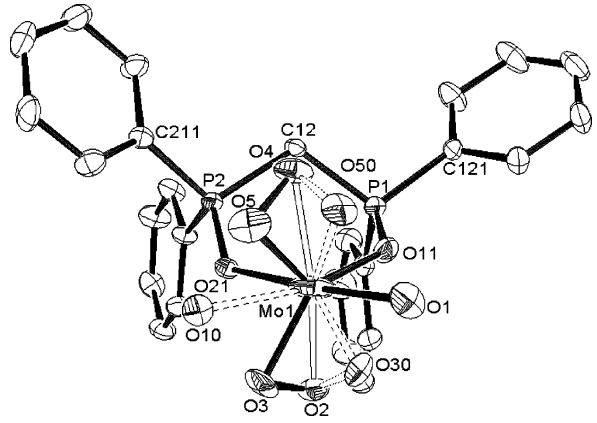

Figure 5. Crystal representation (ORTEP-3[26]) of **9** with selected atom numbering. Thermal ellipsoids are drawn at the 20% probability level. Hydrogen atoms are omitted for clarity. The structure showed positional disorder with 70% major orientation (O1, O2, O3, O4, O5) and 30% minor orientation ((with dashed lines for bonds) O10, O2, O30, O4, O50). Bonds between Mo1 and O2 and Mo1 and O4 are depicted with open lines as these pertain in both forms of the molecule.

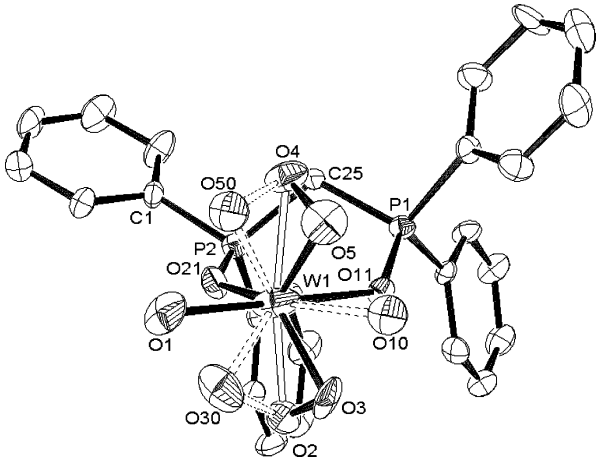

Figure 6. Crystal representation (ORTEP-3[26]) of **10** with selected atom numbering. Thermal ellipsoids are drawn at the 20% probability level. Hydrogen atoms are omitted for clarity. The structure showed positional disorder with 65% major orientation (O1, O2, O3, O4, O5) and 35% minor orientation ((with dashed lines for bonds) O10, O2, O30, O4, O50). Bonds between Mo1 and O2 and Mo1 and O4 are depicted with open lines, as these pertain in both forms of the molecule.

of 1.894(8), 1.813(9), 1.962(7), 1802(12), 1.63(2), and 1.78-(2) Å are shorter than the previously reported values of 1.91−1.99 Å.[31a,32b,34] and the O−O bonds are quite variable at 1.404(13) and 1.420(14) Å for the major (70%) orientation and 1.34(3) and 1.58(3) Å for the minor orientation. Some of these are not in the reported 1.45−1.49 Å range for O−O bond distances.[31a,32b,34a,b,35] The bond parameters about the coordinated $dppmO_2$ ligand are normal, and it is likely that the disorder in the crystal is as a result of 2-fold rotation about this ligand. Evidence for this is also present in the elongated ellipsoid (attempts to resolve this were not successful) for the Mo atom and in the fact that the two Mo−O_{lig} distances were not significantly different. In the related complex containing the monodentate ligand $Mo(O)(O_2)_2(OPMePh_2)_2$, large difference were observed for the M−O_{axial} at 2.326(3) Å compared to the M−$O_{equatorial}$ at 2.063(3) Å.[32b] These differences were apparent in the ^{31}P NMR spectra of a solution of **9** and related **10** as mentioned earlier.

3.3.6. Crystal Structure of 10. Compound **10** was isostructural to compound **9**. The crystal displayed similar disorder of the oxygen atoms of the peroxo and oxo ligands, as shown in Figure 6. Selected bond parameters of **10** are listed in Table 9. The disorder altered the bond distances about the W atom in ways similar to that described for the Mo analogue **9**, and this has resulted in bond data that are not accurate. The 65:35 disorder in **10** and the 70:30 disorder in **9** are further evidence that the disorder arises from the packing preferences of the $dppmO_2$ ligand.

3.4. Olefin Epoxidation Catalysis. Epoxidation of *cis*-cyclooctene was performed in the presence of TBHP or H_2O_2 as an oxidant and some of the title compounds as catalysts, eq 2.

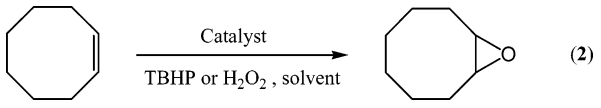

(2)

At room temperature and, if left for 24 h, the oxoperoxomolybdenum catalyst **2** gave a lower percent (i.e., 20%) epoxide conversion than the corresponding dioxo compound **1** (40%) in studies utilizing cyclohexene as the substrate. At increased temperature, the epoxide conversions were in the same range, indicating perhaps that binding of TBHP was reduced with the oxoperoxo **2** compound at lower temperature. It has been found that all compounds assist in the epoxidation of *cis*-cyclooctene. Their extent of conversions

Table 9. Selected Bond Distances (Å) and Angles (deg) for **10** (65% O1, O3, O5:35% O10, O30, O50)

W1−O1	1.835(17)	W1−O30	1.68(3)	O2−O30	1.64(4)	W1−O11	2.208(8)
W1−O3	1.791(13)	W1−O50	1.77(3)	O4−O50	1.35(3)	W1−O21	2.122(9)
W1−O5	1.809(16)	O2−O3	1.460(19)	W1−O2	1.898(11)	O11−P1	1.508(8)
W1−O10	2.16(3)	O4−O5	1.471(18)	W1−O4	1.970(8)	O21−P2	1.497(9)
O1−W1−O2	95.1(7)	O3−W1−O4	140.1(7)	O10−W1−O2	92.8(9)	O30−W1−O50	101.6(17)
O1−W1−O4	99.3(7)	O3−W1−O5	96.6(9)	O10−W1−O4	91.0(9)	O50−W1−O2	155.4(12)
O1−W1−O3	99.9(8)	O3−W1−O11	88.4(5)	O10−W1−O30	93.2(16)	O50−W1−O4	41.9(11)
O1−W1−O5	100.2(8)	O3−W1−O21	132.6(7)	O10−W1−O50	93.6(14)	O50−W1−O11	123.1(12)
O1−W1−O11	164.9(7)	O4−W1−O5	45.6(6)	O10−W1−O11	78.3(8)	O50−W1−O21	96.4(11)
O1−W1−O21	85.3(6)	O4−W1−O11	81.6(4)	O10−W1−O21	158.1(8)	O11−W1−O21	79.9(3)
O2−W1−O3	46.5(6)	O4−W1−O21	83.6(4)	O30−W1−O2	54.2(14)	P1−O11−W1	132.1(5)
O2−W1−O5	142.2(7)	O5−W1−O11	91.2(6)	O30−W1−O4	143.5(14)	P2−O21−W1	137.1(6)
O2−W1−O11	81.5(4)	O5−W1−O21	129.1(6)	O30−W1−O11	134.7(15)	O2−W1−O4	161.5(5)
O2−W1−O21	86.2(4)			O30−W1−O21	103.7(14)		

Table 10. Epoxidation of *cis*-Cyclooctene by Dioxo Compounds in the Presence of TBHP at 55 °C

	cyclooctene epoxide (%)[a]			TOF[b]
catalyst	6 h	13 h	24 h	(mol mol cat^{-1} h^{-1})
$MoCl_2(O)_2(OPMePh_2)_2$ **1**	100	100	100	150
$MoCl_2(O)_2$dppmO_2 **5**	63	91	100	71
$WCl_2(O)_2(OPMePh_2)_2$ **3**	30	43	61	34
$WCl_2(O)_2$dppmO_2 **7**	22	35	52	18

[a] GCMS quantitative (catalyst/substrate/TBHP ratio = 1:100:150), see text for further details. [b] The TOFs were calculated after 30 min reaction time and described as mol epoxide/mol catalyst time (h).

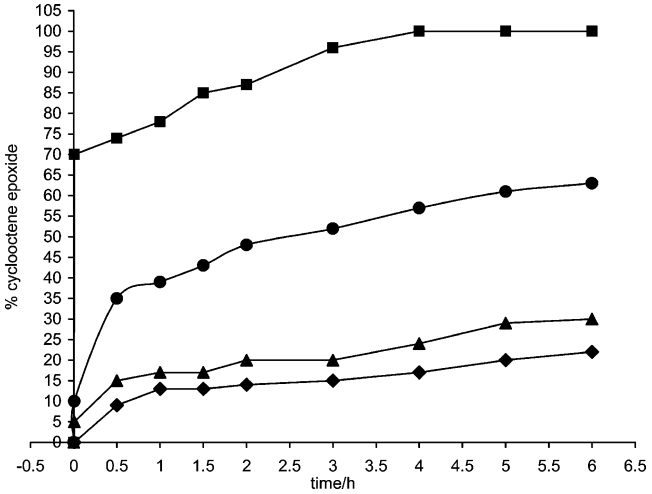

Figure 7. Time-dependent reaction courses of the *cis*-cyclooctene catalytic epoxidation in the presence of TBHP at 55 °C up to 6 h. Key: catalyst **1**, ■; catalyst **5**, ●; catalyst **3**, ▲; catalyst **7**, ◆.

are different, but all reactions are remarkably clean, as only cyclooctene epoxide was produced. The course of epoxidation reactions, employing compounds **1**, **3**, **5**, and **7** as catalysts, are shown in Figure 7, and additional data are summarized in Table 10. Initially, reactions are exothermic and proceed quickly, signifying that an active catalytic species is formed rapidly upon the addition of TBHP. It is noteworthy that blank reactions performed without addition of catalysts result in significant quantities of epoxide, i.e., 55 °C, 24 h, 15%; 70 °C, 13 h, 28%; 90 °C, 6 h, 26% epoxide.

1 is the best catalyst among the four studied judging from the data in Figure 7. Experiments to optimize the catalytic condition were reported previously.[36] The conversion was completed after 4 h at 55 °C. Moreover, we found that the reaction still proceeded rapidly upon the addition of more substrate and oxidizing agent (equal to the initial quantities used) after the first run was completed. However, the catalyst was reduced after the sixth cycle, ca. 500 turnover number. These results indicate that an active catalytic species is still present in the reaction after the first few runs. The lower rate may due to the coordination of *tert*-butyl alcohol (a byproduct) to the catalyst.[14b]

In contrast, **5** resulted in 63% epoxide conversion after 6 h and reached 100% only after 24 h at 55 °C. The dioxo W(VI) analogue, **7**, only converted 52% at 55 °C and 24 h. Attempts to perform the reaction with **7** at higher temperatures resulted in a higher yield, i.e., 22% at 55 °C compared to 70% yield at 90 °C after 6 h. However, extending the reaction time at 90 °C resulted in the decomposition of the added internal standard (i.e., *n*-dibutyl ether). This finding led to a change in the experimental procedure to the extent that the internal standard was added after the reaction was finished, which is different to that reported previously.[7]

The TOF for **1** measured at 5 min is 847 mol mol cat^{-1} h^{-1} which is higher than the 20−600 mol mol cat^{-1} h^{-1} range reported for those dioxomolybdenum(VI) complexes bearing nitrogen base ligands.[9,10] The (η^5-C_5Bz_5)$MoCl(O)_2$ complex is reported to have a TOF of 1200 mol mol cat^{-1} h^{-1}, but this complex is quite moisture sensitive in solution and can be handled under an open atmosphere for only short periods of time in the solid state.[37a] More recently, closely related systems that are not moisture sensitive, mainly because their stable carbonyl precursors can be used, have been developed.[37b−d] On the other hand, the $MoCl_2(O)_2(OPMePh_2)_2$ catalyst is very stable exposed to the atmosphere in either the solid state or in solution with no sign of decomposition.

The tungsten analogue **3** displayed very low catalytic activity. The epoxide conversion was only 30% after 6 h

(34) (a) Bayot, D.; Tinant, B.; Devillers, M. *Inorg. Chim. Acta* **2004**, *357*, 809−816. (b) Sensato, F. R.; Cass, Q. B.; Longo, E.; Zukerman-Schpector, J.; Custodio, R.; Andrés, J.; Hernandes, M. Z.; Longo, R. L. *Inorg. Chem.* **2001**, *40*, 6022−6025. (c) Jacobson, S. E.; Tang, R.; Mares, F. *Inorg. Chem.* **1978**, *17*, 3055−3063. (d) Le Carpentier, P. J.-M.; Schlupp, R.; Weiss, R. *Acta Crystallogr. B* **1972**, *28*, 1278−1288.

(35) (a) Kiraz, C. I. A.; Emge, T. J.; Jimenez, L. S. *J. Org. Chem.* **2004**, *69*, 2200−2202. (b) Hinner, M. J.; Grosche, M.; Herdtweck, E.; Thiel, W. R. *Z. Anorg. Allg. Chem.* **2003**, *629*, 2251−2257. (c) Winter, W.; Mark, C.; Schurig, V. *Inorg. Chem.* **1980**, *19*, 2045−2048. (d) Glas, H.; Spiegler, M.; Thiel, W. R. *Eur. J. Inorg. Chem.* **1998**, 275−281. (e) Martin-Zarza, P.; Gili, P.; Rodriguez-Romero, F. V.; Ruiz-Perez, C.; Solans, X. *Inorg. Chim. Acta* **1994**, *223*, 173−175.

(36) Jimtaisong, A.; Luck, R. L. *J. Cluster Sci.* **2005**, *16*, 167−184.

and 61% after 24 h at 55 °C. At higher temperatures, the rate of epoxidation increased, i.e., 60% epoxide after 6−13 h at 70 °C. However, extending the reaction time at 70 °C to 24 h resulted in a decrease in both epoxide and substrate. Additionally, the reaction accomplished only 70% conversion yield at 90 °C after 6 h and at longer time periods, the quantities of all components in the reaction mixture were diminished. As mentioned previously, compound **7** also showed a lower activity compared to the tungsten monodentate, **3**, and the molybdenum analogue, **5**, see Table 10. Noteworthy, the reaction at 90 °C with **7** resulted in a 70% conversion after 6 h, which is comparable to that found using catalyst **3**. The results in Table 10 are consistent with a situation in which coordination and activation of TBHP is either reduced in the case of **5** (where the bidentate ligand does not dissociate as easily as the monodentate ligands in **1**) or hindered due to restricted dissociation due to the stronger metal to ligand bonds in the W(VI) complexes **3** and **7**.

Other reported dioxo W(VI) complexes, e.g., $WCl_2(O)_2$-(DME),[7] for the epoxidation of *cis*-cyclooctene resulted in only 27% epoxide at 55 °C and 24 h, 36% at 70 °C for 6 h, and 75% at 90 °C and 6 h. The catalytic reactivity of the other $WX_2(O)_2(L)_2$ compounds, where X = Cl or alkyl and L = various bidentate nitrogen donors, have also been reported with fairly low epoxide yields, i.e., about 19% at 70 °C and 6 h and 42% at 90 °C for 6 h.[7] Our W(VI) compounds appear slightly superior for this particular epoxidation reaction.

3.5. Epoxidation Reaction in the Presence of H_2O_2. Hydrogen peroxide is a very attractive green oxidant [38] for various organic compounds, as H_2O is the byproduct.[39] The development of epoxidation catalysts utilizing the H_2O_2 system is constructive for the environment and the CH_3ReO_3 (MTO) catalyst (MTO/H_2O_2/pyridine system) is a good example.[40] In addition to the high cost and moisture sensitivities[41] of the CH_3ReO_3 catalyst compared to the Mo-based catalysts, the fact that a large amount of pyridine is used is also of concern for environmental considerations with the MTO system. Mimoun-type peroxo complexes, MCl_2-$(O)(O_2)(L)_2$ and $M(O)(O_2)_2(H_2O)(L)$, where M = Mo, W, L = hmpa, dmf, have also been examined extensively as stoichiometric catalysts for olefins epoxidation.[4a,42] However, use of or testing of these catalysts in conjunction with H_2O_2 was limited due to their decomposition over the reaction periods. An oxo−tungsten cluster/H_2O_2 system was reported to show great reactivity for olefin epoxidation,[43] and it was concluded that this reaction proceeded via an oxo-peroxo-tungsten active species.[44]

Table 11. Epoxidation of *cis*-Cyclooctene in the Presence of H_2O_2 and CH_3CN Solvent

	cyclooctene epoxide (%)[a]	
catalyst	55 °C 24 h	90 °C 24 h
$MoCl_2(O)_2(OPMePh_2)_2$ **1**	35	20
$WCl_2(O)_2(OPMePh_2)_2$ **3**	70	70

[a] Yield determined from calibration curve; catalyst/substrate/H_2O_2 mole ratio is 1:100:200.

The formation of the oxodiperoxo $M(O)(O_2)_2$dppmO_2 compounds in the presence of an excess H_2O_2, as shown in Scheme 1, suggested that these complexes may be stable to catalyst in the presence of H_2O_2.

To optimize conditions, the reactions were studied in various solvents. Toluene or benzene as solvents resulted in biphasic reactions, and no epoxide formation was observed. In dichloromethane, the epoxidation reaction resulted in a small quantity of epoxide at room temperature. However, reactions at temperatures higher than 40 °C were not possible. Catalysis in acetonitrile did result in the formation of appreciable quantities of epoxide product at temperatures greater than 40 °C, as shown in Table 11.

It is noteworthy to mention that an alkali-catalyzed epoxidation of cyclohexene using a nitrile as a co-reactant has been previously reported.[45] The reported reaction was performed in methanol at a pH of 7.5−8.0. The addition of NaOH solution was required in order to control the pH of the system. It was suggested that hydrogen peroxide reacts with a nitrile to generate a peroxycarboximidic acid (RC-(NH)COOH) intermediate, which then reacts with the olefins to produce the epoxide.[45] In our system with acetronitrile, a blank reaction conducted in the absence of catalyst did not yield epoxide. This suggests that, in our system, a peroxycarboximidic acid is not the active catalytic intermediate. Catalyst in acetonitrile is possible perhaps because of its solubilizing attribute, which provides for a miscible mixture of water-soluble and water-insoluble materials.

We were initially reluctant to use alcoholic solvents, since in the TBHP system, the reaction rate in alcohols is relatively low compared with noncoordinating chlorinated solvents or

(37) (a) Abrantes, M.; Santos, A. M.; Mink, J.; Kühn, F. E.; Romão, C. C. *Organometallics* **2003**, *22*, 2112−2118. (b) Freund, C.; Abrantes, M.; Kühn, F. E. *J. Organomet. Chem.* **2006**, *691*, 3718−3729. (c) Sakthivel, A.; Zhao, J.; Hanzlik, M.; Chiang, A. S. T.; Herrmann, W. A.; Kühn, F. E. *Adv. Synth. Catal.* **2005**, *347*, 473−483. (d) Zhao, J.; Herdtweck, E.; Kühn, F. E. *J. Organomet. Chem.* **2006**, *691*, 2199−2206.

(38) Noyori, R.; Aoki, M.; Sato, K. *Chem. Commun.* **2003**, *16*, 1977−1986.

(39) (a) Jones, C. W. In *Applications of Hydrogen Peroxide and Derivatives*; Clark, J. H., Ed.; Royal Society of Chemistry, Thomas Graham House, Cambridge, 1999. (b) Centi, G.; Cavani, F.; Trifirò, F. S*elective oxidation by Heterogeneous Catalysis*; Kluwer Academic/Plenum Publishers: New York, 2001.

(40) Rudolph, J.; Reddy, K. L.; Chiang, J. P.; Sharpless, K. B. *J. Am. Chem. Soc.* **1997**, *119*, 6189−6190.

(41) (a) The conclusion that MTO is moisture sensitive is based on our research where, if MTO was subjected to water for 4 h, the substance referred to as "poly-CH_3ReO_3" is obtained. See Wang, G.; Jimtaisong, A.; Luck, R. L. *Organometallics* **2004**, *23*, 4522−4525. (b) Others have reported on the reactivity of CH_3ReO_3 under acidic and basic conditions. See Romão, C. C.; Kühn, F. E.; Herrmann, W. A. *Chem. Rev.* **1997**, *97*, 3197−3246.

(42) Mimoun, H.; Seree de Roch, I.; Sajus, L. *Tetrahedron* **1970**, *26*, 37−50.

(43) (a) Lane, B. S.; Burgess, K. *Chem. Rev.* **2003**, *103*, 2457−2473. (b) Kozhevnikov, I. V. *Chem. Rev.* **1998**, *98*, 171−198. (c) Mizuno, N.; Yamaguchi, K.; Kamata, K. *Coord. Chem. Rev.* **2005**, *249*, 1944−1956.

(44) (a) Salles, L.; Aubry, C.; Thouvenot, R.; Robert, F.; Dorémieux-Morin, C.; Chottard, G.; Ledon, H.; Jeannin, Y.; Brégeault, J.-M. *Inorg. Chem.* **1994**, *33*, 871−878. (b) Aubry, C.; Chottard, G.; Platzer, N.; Brégeault, J.-M.; Thouvenot, R.; Chauveau, F.; Huet, C.; Ledon, H. *Inorg. Chem.* **1991**, *30*, 4409−4415.

(45) Payne, G. B.; Deming, P. H.; Williams, P. H. *J. Org. Chem.* **1961**, *26*, 659−663.

Table 12. Epoxidation of *cis*-Cyclooctene with Catalysts in the Presence of H_2O_2 in Ethanol Solvent

		cyclooctene epoxide (%)[a]	
catalyst	no. of catalyst	1 h	6 h
$MoCl_2(O)_2(OPMePh_2)_2$	**1**	none observed	43
$MoCl_2(O)_2dppmO_2$	**5**	none observed	26
$WCl_2(O)_2(OPMePh_2)_2$	**3**	37	90
$WCl_2(O)(O_2)(OPMePh_2)_2$	**4**	50	97
$WCl_2(O)_2dppmO_2$	**7**	51	98
$WCl_2(O)(O_2)dppmO_2$	**8**	40	98
$W(O)(O_2)_2dppmO_2$	**10**	39	90

[a] GCMS quantitative using an internal standard technique; catalyst/substrate/H_2O_2 mole ratio is 1:100:150. $T = 70$ °C.

benzene.[46] However, we have discovered that ethanol is a much more suitable solvent than acetonitrile for the epoxidation of *cis*-cyclooctene with hydrogen peroxide (i.e., 100% epoxide when using catalyst **3**, 78 °C, 24 h). The blank reaction (i.e., without catalyst) did not result in any epoxide being produced. Furthermore, the quantity of hydrogen peroxide at different ratios to substrate was varied, and while 1 equiv of H_2O_2 resulted in 77% conversion, increasing this to 1.5 and 2 equiv of H_2O_2 resulted in an increase in epoxide production to 90 and 92%, respectively.

The results from the epoxidation of *cis*-cyclooctene with the EtOH/H_2O_2 system are presented in Table 12. Interestingly, it has been found that **5,** which was initially less reactive than **1**, after 24 h gave a slightly higher epoxide yield (75%) than **1** as catalyst (62%). Some catalysts were also tested for a second reaction cycle under identical conditions, that is, by charging with an extra 100 mol equiv of substrate and 1.5-fold of H_2O_2. The epoxidation reaction did not proceed for a second run when **3** was used. However, with **7**, the epoxidation reaction continued, albeit at a lower rate after the third run, and the reaction was fairly slow for the fourth cycle. These results may well be due to the less dissociable, bidentate $dppmO_2$ ligand in these compounds as compared to the monodentate complexes where the monodentate ligands may have been displaced by EtOH.

Interestingly, in EtOH, the W-based catalysts gave higher epoxide conversions than the Mo-based catalysts, opposite to the TBHP system reported above. The stability of the W-based catalysts may be related to the increase in the general M−L bond strength from the first row down to the third row transition metals. Therefore, the tungsten catalytic species function better in the presence of a strong oxidant such as H_2O_2 and the EtOH solvent, where the dissociation of ligand(s) may result in premature decomposition of the catalyst.

3.6. Properties of Catalysts in Ethanol. Using ^{31}P NMR spectroscopy, we have assessed the stability of the catalysts in EtOH under similar conditions to those used in the epoxidation reactions, i.e., 70 °C for 6 h. These spectra revealed complete dissociation of the $OPMePh_2$ ligand for compound **3**. The spectra for the bidentate compounds, **5** and **7**, contained peaks assigned to the original compounds and an extra peak in the high-field direction, suggesting some dissociation may have taken place. The addition of excess 30% H_2O_2 (i.e., 150 mol equiv) into an ethanol solution of compound **5** (or **7**) under identical conditions to that for the catalytic studies results in the formation of compounds **9** (or **10**) and the presence of uncoordinated $dppmO_2$ ligand. These results indicated that the oxodiperoxo species might be an intermediate in the epoxidation reaction. However, a stoichiometric reaction of an oxodiperoxo species (i.e., **9** or **10**) and *cis*-cyclooctene initially produced only a small amount of epoxide. At longer reaction times, the concentration of epoxide remained constant and another signal assignable to the corresponding diols was also detected, both being in much smaller quantities compared to the reactant.

4. Conclusions

Several new complexes of dioxo or oxoperoxo Mo(VI) and W(VI) bearing phosphine oxide ligands have been synthesized and assessed for their catalytic epoxidation applicability of *cis*-cyclooctene. The compounds were easily synthesized and produced in good yield. All compounds are stable and can be handled under open atmospheric conditions. The addition of an excess of H_2O_2 to the dioxo of the bidentate phosphine oxide complexes $MCl_2(O)_2dppmO_2$, where M = Mo or W, resulted in the formation of the corresponding oxodiperoxo $M(O)(O_2)_2dppmO_2$, whereas the dioxo of the monodentate phosphine oxide complexes decomposed and do not afford the corresponding oxodiperoxo species under the same conditions. The epoxidation of *cis*-cyclooctene using the synthesized compounds as catalysts has been examined. W-based catalysts showed a lower reactivity than Mo-based catalysts in the presence of TBHP as the oxidant. However, the W-based catalysts showed a superior reactivity over the Mo-based catalysts when H_2O_2 was the oxidant, and ethanol appeared to be the best solvent for the H_2O_2 system. Finally, it must be noted that these catalytic epoxidation reactions were very clean. An epoxide was the only product detected. The H_2O_2-based catalytic epoxidation is noteworthy with respect to environmental considerations because H_2O is produced. The use of ethanol as solvent is also advantageous because it is considered to be less toxic and more environmentally friendly than chlorinated or nonpolar solvents.

Acknowledgment. This work was supported by Michigan Technological University (MTU). We acknowledge the contributions of reviewers and Professor Judith Perlinger of the Department of Civil and Environmental Engineering at MTU for helpful suggestions and comments. We thank Ms. Soumyashree Sreehari for her assistance in obtaining the ^1H NMR spectra.

Supporting Information Available: X-ray crystallographic data in standard CIF format for compound **3**, **4**, **5**, **7**, **9**, and **10**; ^1H NMR spectra of compounds **3**−**10**. This material is available free of charge via the Internet at http://pubs.acs.org.

IC061455D

(46) Sheldon, R. A.; Van Doorn, J. A.; Schram, C. W. A.; De Jong, A. J. *J. Catal.* **1973**, *31*, 438−443.